

The organotellurium compound ammonium trichloro(dioxoethylene-*o,o'*)tellurate reacts with homocysteine to form homocystine and decreases homocysteine levels in hyperhomocysteinemic mice

Eitan Okun^{1,*}, Yahav Dikshtein^{1,*}, Alon Carmely¹, Hagar Saida¹, Gabi Frei¹, Ben-Ami Sela², Lydia Varshavsky¹, Asher Ofir³, Esthy Levy³, Michael Albeck³ and Benjamin Sredni¹

¹ CAIR Institute, The Safdié AIDS and Immunology Research Center, Bar-Ilan University, Ramat-Gan, Israel

² Institute of Chemical Pathology, Chaim Sheba Medical Center, Tel-Hashomer, Israel

³ Department of Chemistry, Faculty of Exact Sciences, Bar-Ilan University, Ramat-Gan, Israel

Keywords

AS101; homocysteine; hyperhomocysteinemia; organotellurium; tellurium

Correspondence

B. Sredni, Safdié Institute for AIDS and Immunology Research, The Mina & Everard Goodman Faculty of Life Sciences, Bar-Ilan University, Ramat-Gan 52900, Israel
Fax: +972 36356041
Tel: +972 35318250
E-mail: srednib@mail.biu.ac.il, srednib@gmail.com

*These authors contributed equally to this work

(Received 21 November 2006, revised 4 April 2007, accepted 24 April 2007)

doi:10.1111/j.1742-4658.2007.05842.x

Ammonium trichloro(dioxoethylene-*o,o'*)tellurate (AS101) is an organotellurium compound with pleiotropic functions that has been associated with antitumoral, immunomodulatory and antineurodegenerative activities. Tellurium compounds with a +4 oxidation state, such as AS101, react uniquely with thiols, forming disulfide molecules. In light of this, we tested whether AS101 can react with the amino acid homocysteine both *in vitro* and *in vivo*. AS101 conferred protection against homocysteine-induced apoptosis of HL-60 cells. The protective mechanism of AS101 against homocysteine toxicity was directly mediated by its chemical reactivity, whereby AS101 reacted with homocysteine to form homocystine, the less toxic disulfide form of homocysteine. Moreover, AS101 was shown here to reduce the levels of total homocysteine in an *in vivo* model of hyperhomocysteinemia. As a result, AS101 also prevented sperm cells from undergoing homocysteine-induced DNA fragmentation. Taken together, our results suggest that the organotellurium compound AS101 may be of clinical value in reducing total circulatory homocysteine levels.

Homocysteine is a thiol-containing amino acid synthesized in mammals/humans as part of the normal metabolism of the essential amino acid methionine. Studies conducted over the past three decades have shown that high levels of homocysteine in the plasma (hyperhomocysteinemia, i.e. $> 15 \mu\text{mol}\cdot\text{L}^{-1}$) constitute a risk factor for cardiovascular diseases and stroke [1]. Elevated homocysteine is also a risk factor for several neurodegenerative disorders, such as dementia [2],

Alzheimer's disease [3], and Parkinson's disease [4]. As elevated homocysteine is associated with an increasing number of pathologies, the regulation of homocysteine levels is of clinical importance.

Several factors contribute to elevated homocysteine levels: (a) genetic disorders stemming from mutations in the enzymes involved in homocysteine remethylation to methionine (e.g. 5,10-methylenetetrahydrofolate reductase) [5], or mutations in homocysteine catabolism

Abbreviations

AS101, ammonium trichloro(dioxoethylene-*o,o'*)tellurate; ddw, double-deionized water; DEVD, Ac-benzyloxycarbonyl aspartyl glutamylvalylaspartic acid; DFI, DNA fragmentation index; FACS, fluorescence-activated cell sorter; Nbs₂, 5,5'-dithiobis(2-nitrobenzoic acid); PI, propidium iodide; pNA, *p*-nitroaniline; RP, reaction product; SCSA, sperm chromatin structure assay.

(e.g. cystathionine- β -synthase) [6]; (b) acquired disorders arising from lack of metabolites such as folic acid [7] and cobalamin (vitamin B₁₂) [8], which prevents its turnover to methionine, or lack of pyridoxine (vitamin B₆), which prevents its turnover to cysteine [9]; and (c) acquired disorders related to lifestyle choices, such as smoking [10], excessive coffee consumption [11], and alcoholism [12].

Currently, there are several homocysteine-lowering agents available. Cobalamin and vitamin B₆ are administered to patients with hyperhomocysteinemia caused by a lack of these factors, and vitamin B₆ is also given to patients with homocystinuria caused by cystathionine- β -synthase deficiency. Folic acid is given to healthy subjects with high homocysteine levels, regardless of the cause. Three thiol-containing drugs have been shown to suppress plasma homocysteine levels: D-penicillamine, N-acetylcysteine, and 2-mercaptoethanesulfonate [13–15]. Despite these treatments, homocysteine levels remain elevated in some patients. In healthy individuals, the urinary excretion of homocysteine is less than 10 $\mu\text{mol}\cdot\text{day}^{-1}$, which is less than 1% of the daily homocysteine turnover in plasma [35]. Metabolic homocysteine removal is mediated by the renal parenchymal cells; homocysteine can be taken up from the glomerular filtrate by the proximal renal tubular cells [36]. All the trans-sulfuration as well as remethylation enzymes are present in these kidney cells.

A large body of evidence suggests that the free -SH form of homocysteine is involved in NO blockage, atherogenic activity, and other adverse vascular activities. Homocysteine, in its oxidized form, bound to either albumin or glutathione, or as a mixed disulfide linked to other homocysteine or cysteine molecules, does not appear to mediate the negative activities associated with free homocysteine. Hence, increased conversion of homocysteine to homocystine might increase renal clearance and prevent the adverse effects of high free homocysteine levels.

5,10-Methylenetetrahydrofolate reductase-deficient mice have significantly higher levels of plasma homocysteine, due to their reduced ability to remethylate homocysteine to methionine. These mice were characterized by abnormal spermatogenesis and male infertility, factors attributed to the overall effect of methylation defects rather than high homocysteine levels [16]. A more recent study that examined thiol status in subfertile couples found that homocysteine levels were inversely associated with fertility outcome [17].

The nontoxic compound ammonium trichloro(dioxoethylene-*o,o'*) tellurate (AS101) is a synthetic organotellurium compound with multiple biological activities. Most of these activities have been primarily

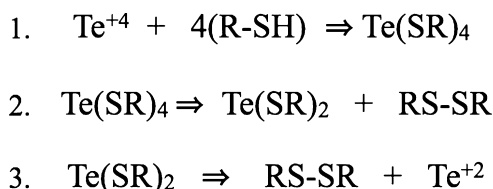
attributed to the direct inhibition of the cytokine interleukin-10 [18–20]. This immunomodulatory property was found to be crucial for the clinical activities of AS101, which exhibits protective effects in a parasite model [21], in autoimmune diseases [22], and in septic mice [23]. In addition, AS101 exhibits a clear antitumoral effect on a variety of mouse and human tumor models [24,25]. Recently AS101 was shown to exert neuroprotective effects in animal models of Parkinson's disease [41] and in ischemic brain stroke [42].

The various activities of AS101 are attributed to its tellurium atom. The chalcogen family of atoms, also known as periodic table group 16, includes oxygen, sulfur, selenium, tellurium, and polonium. These elements share the same electron arrangement (each has six free electrons in its outer shell), enabling them to readily interact with each other to form disulfide-like bonds. The ability of AS101 to react with thiol-containing molecules was reported by Albeck *et al.* [26]. Tellurium compounds with a +4 oxidation state, such as AS101, interact readily with nucleophiles such as alcohols, thiols, and carboxylates, yielding (Nu)₄Te products, or, in our case, Te(SR)₄ (Scheme 1, Reaction 1). The Te(SR)₄ product undergoes an oxidation–reduction reaction according to: $\text{Te}(\text{SR})_4 \Rightarrow \text{Te}(\text{SR})_2 + \text{RSSR}$ (Scheme 1, Reaction 2). Te(SR)₂ may further react to form a second disulfide as well as a tellurium atom with a +2 oxidation state (Scheme 1, Reaction 3). The aim of this study was to investigate whether these reactions could occur *in vivo* to ablate homocysteine when present at elevated levels. We show here that AS101 reacted with homocysteine, causing its oxidation to homocystine, and that it can also lower elevated homocysteine levels *in vivo*. This work provides a promising new therapy for reducing homocysteine levels using this nontoxic organotellurium compound, which is already in clinical trials in cancer and Parkinson's disease at different stages.

Results

AS101 reduced homocysteine-induced apoptosis of HL-60 cells

The HL-60 cell line model system for homocysteine toxicity used in this study was not intended to provide insights into the pathophysiologic effects of homocysteine *in vitro* or *in vivo*, but rather a platform to determine whether AS101 was able to protect cells from elevated levels of homocysteine. We first tested the effect of AS101 on apoptosis in HL-60 cells in the presence of homocysteine in the medium. D,L-Homocysteine (6 mM) increased the percentage of hypodiploid



Scheme 1. AS101 oxidized thiol groups (–SH) to produce RS–SR disulfide molecules in three steps. Reaction (I): tellurium compounds with a +4 oxidation state, such as AS101, interact readily with nucleophiles such as thiols, yielding $\text{Te}(\text{SR})_4$. Reaction (II): the resulting product undergoes an oxidation–reduction reaction according to the following reaction: $\text{Te}(\text{SR})_4 \Rightarrow \text{Te}(\text{SR})_2 + \text{RSSR}$. Reaction (III): $\text{Te}(\text{SR})_2$ may react further to form a second disulfide as well as a tellurium atom with a +2 oxidation state.

cells in the promyelocytic cell line HL-60, as previously demonstrated for homocysteine thiolactone [30]. Like homocysteine thiolactone, homocysteine induced caspase-3-dependent apoptosis in HL-60 cells. Significantly elevated caspase-3 activity levels were observed 3 h after homocysteine addition (Fig. 1A). After 4 h, apoptotic cells appeared to be hypodiploid cells, i.e. cells during apoptotic DNA degradation (Fig. 1B). These hypodiploid cells exhibited an 8.5 ± 3.8 -fold increase in their number as compared to control cells at 6 h after D,L-homocysteine addition, whereas longer incubation periods resulted in extensive apoptosis and cell death. Therefore, all subsequent analyses were performed at a 6 h time point. Addition of AS101 together with D,L-homocysteine resulted in reduced caspase-3 activity and apoptosis levels (Fig. 1C,D, respectively). PARP1, a cleavage substrate of caspase-3 that is inactive once cleaved, was used as another indirect marker for caspase-3-mediated apoptosis. Cleaved PARP1 and the active cleaved form of caspase-3 were both reduced in AS101 and D,L-homocysteine-treated cells, as shown using western blotting (Fig. 2A,B, respectively).

AS101 promoted homocysteine conversion to homocystine

We next used several approaches to determine whether AS101 was able to convert homocysteine to homocystine. Using Raman spectrometry, a method that detects specific atoms in a chemical bond by measuring its vibrational energy state, we analyzed D,L-homocysteine and the *in vitro* reaction product (RP) of AS101 and D,L-homocysteine. Whereas homocysteine showed a distinct peak for its S–H bond ($2550\text{--}2600\text{ cm}^{-1}$) (Fig. 3A), the RP completely lost its S–H bond and gained a new S–S bond instead (430--

550 cm^{-1}) (Fig. 3B). None of these peaks was evident when AS101 alone was analyzed (data not shown). The Raman spectrum for the RP was similar to that of homocystine [37,38]. Next, H^1 -NMR analysis was utilized to identify specific hydrogens in homocysteine and its RP with AS101. As homocysteine is composed of two homocysteine molecules, equivalent hydrogens in both molecules possess similar magnetic resonance attributes, so the H^1 -NMR spectra for homocysteine and homocystine are very similar [37]. H^1 -NMR data (300 MHz, D_2O) analysis of the RP of homocysteine and AS101 resulted in three signals: δ (p.p.m.) = 3.87 (dt, 1 Ha, *CH), 2.84 (m, 2 Hc, CH_2SH), and 2.29 (m, 2 Hb, CH_2). These signals were similar to those measured for homocysteine: H^1 -NMR data (300 MHz, D_2O) δ (p.p.m.) = 3.86 (dd, 1 Ha, *CH), 2.62 (m, 2 Hc, CH_2SH), and 2.13 (m, 2 Hb, CH_2). The similar H^1 -NMR spectra of both homocysteine and its RP with AS101 support our hypothesis that AS101 oxidizes homocysteine to homocystine. The predicted H^1 -NMR spectra for both homocysteine and homocystine, as calculated using CHEMDRAW ULTRA 9.0 software, are similar: δ (p.p.m.) = 3.49 (1 H, *CH), 2.56 (2 H, CH_2SH), and 2.08 (2 H, CH_2). For H^1 -NMR measurements, the hydrogens tagged as a–c are shown on the homocysteine molecule in Fig. 3A.

Next, we analyzed free thiols using the quantitative 5,5'-dithiobis(2-nitrobenzoic acid) (Nbs_2) reagent, which reacts with free thiol (–SH) groups. This analysis also confirmed that whereas homocysteine had a free thiol, the RP was devoid of a free –SH group (Fig. 3C). The reaction of homocysteine occurred within minutes, as measured using Nbs_2 (Fig. 3D).

MS is an analytical technique used to determine the composition of a physical sample by generating a mass spectrum representing the masses of sample components. We used high-resolution MS to determine the composition of the RP of AS101 and homocysteine. The calculated M_r of homocysteine is 267.047, whereas the measured M_r of the RP was 267.049 (Fig. 3F). The similar H^1 -NMR information and the lack of free SH groups in the RP, in addition to the M_r determined by mass spectra, prove that the RP of AS101 and homocysteine is homocystine.

In addition to these four analytical methods, we used another indirect biochemical approach to determine the effect of AS101 on homocysteine. This assay was based on the ability of homocysteine to induce dissociation of IgG molecules. Rabbit IgG incubated with homocysteine overnight *in vitro* with or without AS101 was electrophoresed on a gel. The gel was subsequently stained using silver staining. The results showed that whereas homocysteine disassembled IgG

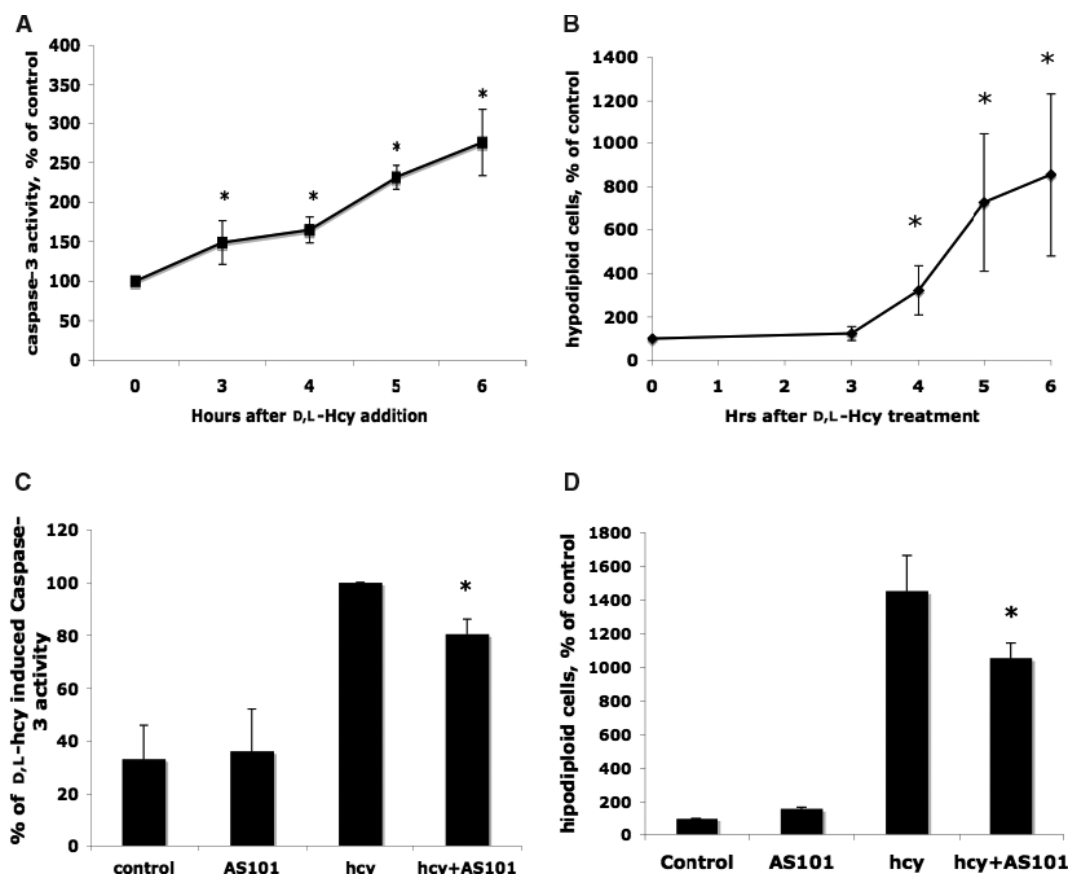


Fig. 1. (A) Kinetic measurement of homocysteine-induced caspase-3 activation in HL-60 cells. HL-60 cells were incubated with 6 mM D,L-homocysteine for 3–6 h. Cells were then harvested and lysed, and 50 μ g of protein was incubated in a 96-well plate with the caspase-3 substrate DEVD-pNA (50 μ M) for 6 h. Plates were then analyzed at a wavelength of 405 nm, using an ELISA reader (680 Microplate Absorbance Reader). The results presented are from at least three repeated experiments. (B) Kinetic measurement of homocysteine-induced apoptosis in HL-60 cells. HL-60 cells were incubated with 6 mM D,L-homocysteine for 3–6 h. Cells were then harvested, fixed, and stained with PI for hypodiploid DNA analysis using a fluorescence-activated cell sorter (FACS). Results are shown as percentage of control (untreated) cells, which, in all experiments, exhibited $4 \pm 2\%$ apoptosis. The results presented are from at least three repeated experiments. (C) AS101 reduces D,L-homocysteine-induced caspase-3 activation. HL-60 cells were incubated with or without 6 mM D,L-homocysteine in the presence or absence of $2.5 \mu\text{g}\cdot\text{mL}^{-1}$ AS101 for 6 h. Cells were then harvested and lysed, and 50 μ g of protein was incubated in a 96-well plate with the caspase-3 substrate DEVD-pNA (50 μ M) for 6 h. Plates were then analyzed at a wavelength of 405 nm using an ELISA reader (680 Microplate absorbance reader). (D) AS101 reduced D,L-homocysteine-induced apoptosis. HL-60 cells were incubated with 6 mM D,L-homocysteine for 6 h. AS101 ($2.5 \mu\text{g}\cdot\text{mL}^{-1}$) was added either with or without homocysteine. Cells were then harvested, fixed, and stained with PI for hypodiploid DNA analysis using a FACS. Results are expressed as the percentage of control (untreated) cells. Error bars represent the SD from three different experiments in duplicate. * $P < 0.05$.

in a dose-dependent manner, AS101 prevented this effect (Fig. 3E).

AS101 decreased total homocysteine but not total cysteine levels in hyperhomocysteinemic mice

The ability of AS101 to inhibit homocysteine was next tested *in vivo*. C57bL/6 mice were divided into four experimental groups: (a) regular water with NaCl/P_i injections ($n = 8$); (b) regular water with AS101 ($1.5 \mu\text{g}\cdot\text{g}^{-1}$) injections ($n = 8$); (c) D,L-homocysteine

($200 \text{ mg}\cdot\text{kg}^{-1}\cdot\text{day}^{-1}$) in the drinking water with NaCl/P_i injections ($n = 8$); and (d) D,L-homocysteine ($200 \text{ mg}\cdot\text{kg}^{-1}\cdot\text{day}^{-1}$) in the drinking water with AS101 ($1.5 \mu\text{g}\cdot\text{g}^{-1}$) injections ($n = 8$). Injections were administered every other day during 8 weeks. Blood was then collected in order to measure total plasma homocysteine and cysteine levels using HPLC. In animals that received D,L-homocysteine in the water, AS101 treatment significantly reduced total homocysteine levels from $22.4 \pm 7.5 \mu\text{M}$ to $12.6 \pm 3.4 \mu\text{M}$ (Fig. 4A). AS101 treatment did not significantly change total cysteine levels in

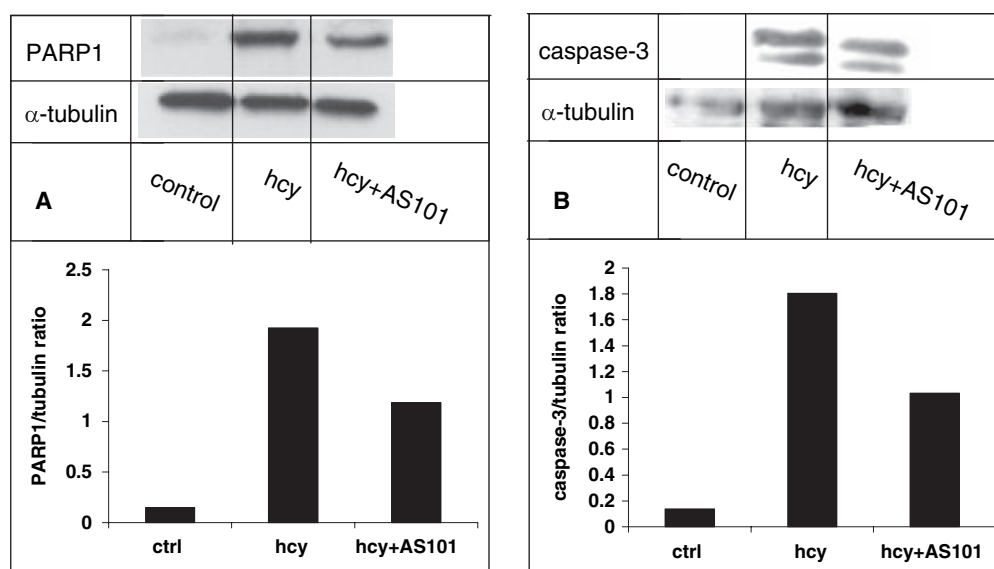


Fig. 2. (A) AS101 reduced D,L-homocysteine-induced PARP1 cleavage. HL-60 cells were incubated with 6 mM D,L-homocysteine for 6 h in the presence of AS101 ($2.5 \mu\text{g}\cdot\text{mL}^{-1}$). Cells were then lysed, and lysates were electrophoresed, blotted onto nitrocellulose membranes, and incubated with antibody against cleaved PARP1. Results are representative of at least three repeated experiments. (B) AS101 reduced D,L-homocysteine-induced caspase-3 activation. HL-60 cells were incubated with 6 mM D,L-homocysteine for 6 h in the presence of AS101 ($2.5 \mu\text{g}\cdot\text{mL}^{-1}$). Cells were then lysed, and lysates were electrophoresed, blotted onto nitrocellulose membranes, and incubated with antibody against cleaved caspase-3. Results are representative of at least three repeated experiments. * $P < 0.05$.

either normally fed mice ($148.7 \pm 13.8 \mu\text{M}$ in NaCl/ P_i -treated mice vs. $133.0 \pm 21.1 \mu\text{M}$ in AS101-treated mice) or in homocysteine-fed mice ($137.4 \pm 17.9 \mu\text{M}$ in NaCl/ P_i -treated mice vs. $122.1 \pm 12.4 \mu\text{M}$ in AS101-treated mice) (Fig. 4B) ($P < 0.05$).

AS101 prevented DNA degradation in sperm cells of hyperhomocysteinemic mice

Sperm cells recovered from testes of sacrificed hyperhomocysteinemic mice were analyzed for fragmented DNA content. DNA fragmentation, expressed as percentage DFI, had increased from $4.9\% \pm 1.2\%$ in control animals to $16.5\% \pm 4.4\%$ in D,L-homocysteine-fed ($200 \text{ mg}\cdot\text{kg}^{-1}\cdot\text{day}^{-1}$) hyperhomocysteinemic mice. This elevation was abrogated by AS101 treatment ($1.5 \mu\text{g}\cdot\text{g}^{-1}$), and the value was reduced to $4.7\% \pm 0.64\%$ (Fig. 5) ($P < 0.05$).

Discussion

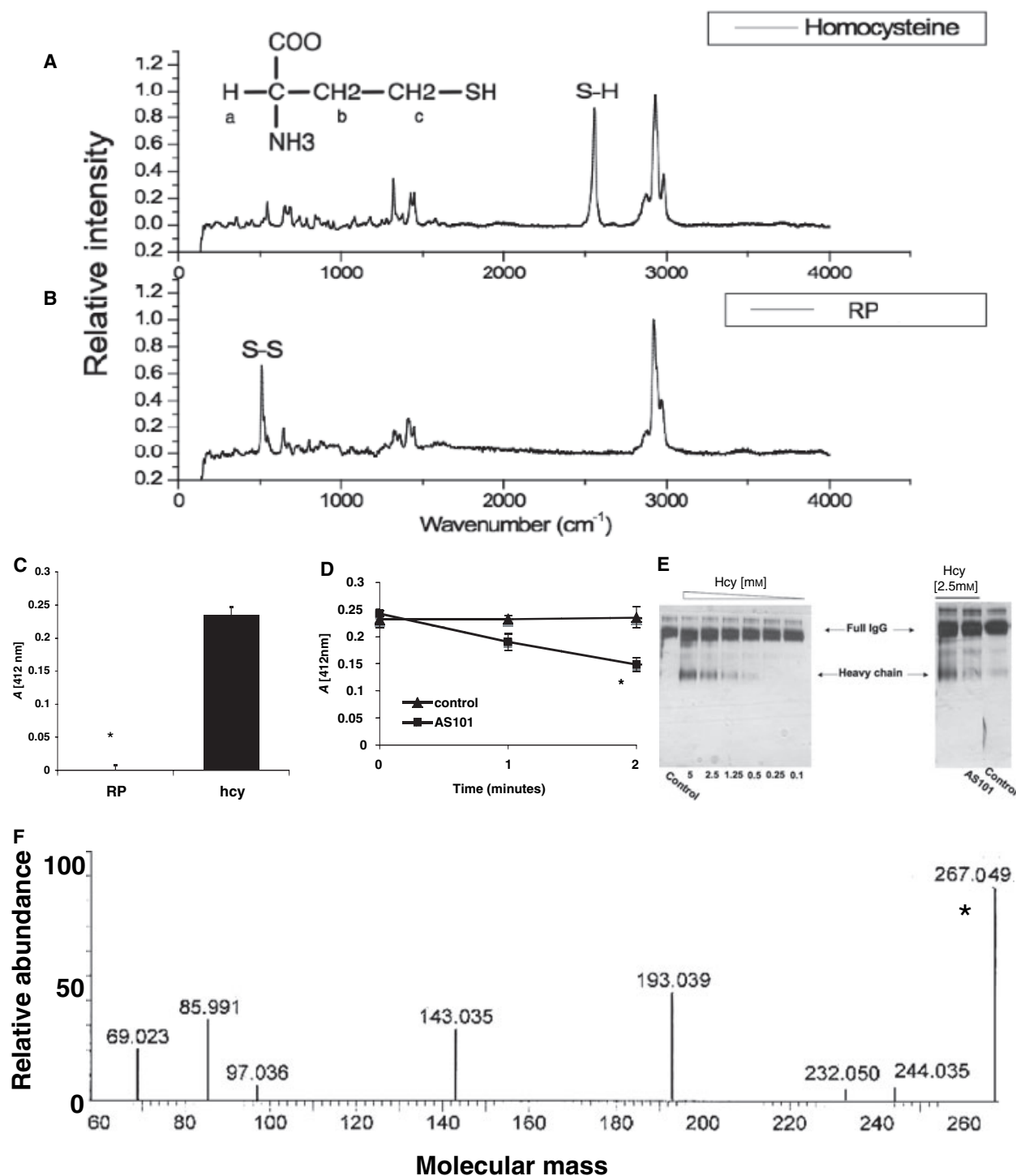
Accumulating evidence suggests that even mild elevations in homocysteine levels are a marker for several pathologies, notably cardiovascular and neurodegenerative disorders, and several homocysteine-reducing agents, such as vitamin B₆, vitamin B₁₂, and folic acid, have been described. N-Acetylcysteine was also evaluated as a possible homocysteine-reducing agent,

although the mechanism for its activity is not entirely clear [31]. Not all hyperhomocysteinemic patients respond to these treatments, probably due to the fact that, except for N-acetylcysteine, these agents act through the body's own metabolic routes. In cases where metabolic abnormalities are the cause of the hyperhomocysteinemia, current treatments are inadequate.

Organotellurium compounds react uniquely with thiols. Tellurium compounds with a +4 oxidation state, such as $\text{Te}(\text{OR})_4$, readily interact with thiols, yielding $(\text{Nu})_4\text{Te}$ products. Further oxidation–reduction reactions, such as $\text{Te}(\text{SR})_4 \Rightarrow \text{Te}(\text{SR})_2 + \text{RSSR}$, subsequently occur. $\text{Te}(\text{SR})_2$ may further react to form a second disulfide and an inorganic tellurium compound [26]. Interestingly, serum selenium levels were recently shown to be associated with plasma homocysteine concentrations in elderly humans [32]. This led us to examine whether the organotellurium compound AS101 can be utilized as a general homocysteine-reducing agent. In this study, we initially used a well-studied *in vitro* model for homocysteine toxicity in the HL-60 cell line [23]. This model was used for analysis of the effect of AS101 on homocysteine under culture conditions, but not to study the pathophysiologic effects of homocysteine that occur *in vivo*, as the concentrations (6 mM *in vitro* as opposed to 15–100 μM *in vivo*) were much higher *in vitro*.

To establish the experimental system, we determined the kinetics of caspase-3 induction in these cells (Fig. 1A), as well as the apoptotic process induced by homocysteine, expressed as percentage of hypodiploid cells (Fig. 1B). The addition of AS101, together with homocysteine, at a total incubation time of 6 h,

resulted in reduction of caspase-3 activity (Fig. 1C) and apoptosis (Fig. 1D). Through reduction of the apoptotic process, the levels of cleaved PARP1, a caspase-3 substrate, and caspase-3 itself were reduced, as shown by western blotting (Fig. 2A,B, respectively).



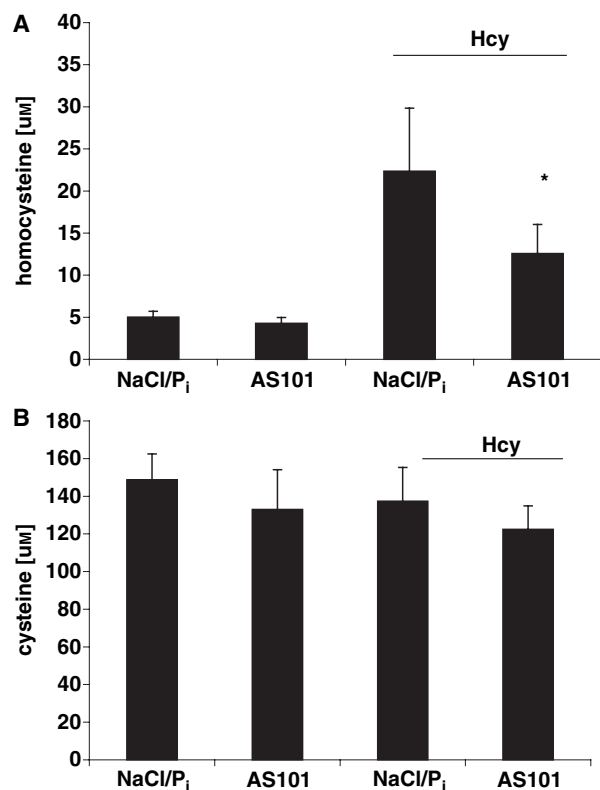


Fig. 4. AS101 lowers total homocysteine but not total cysteine in mice fed D,L-homocysteine. C57BL/6 mice were divided into four groups and treated with: (A) regular water with NaCl/P_i injections ($n = 8$); (B) regular water with AS101 ($1.5 \mu\text{g}\cdot\text{g}^{-1}$) injections ($n = 8$); (C) D,L-homocysteine ($200 \text{ mg}\cdot\text{kg}^{-1}\cdot\text{day}^{-1}$) in the drinking water with NaCl/P_i injections ($n = 8$); and (D) D,L-homocysteine ($200 \text{ mg}\cdot\text{kg}^{-1}\cdot\text{day}^{-1}$) in the drinking water with AS101 ($1.5 \mu\text{g}\cdot\text{g}^{-1}$) injections ($n = 8$). Injections were administered every other day during the 8 weeks of homocysteine administration. Mice were then killed with excess CO₂, and blood plasma was obtained. Plasma samples were analyzed for homocysteine (a) and cysteine (b) levels using HPLC. * $P < 0.05$. The data shown represent the averages of three different experiments performed in duplicate; error bars indicate SD.

In order to find a possible mechanism for the direct and rapid effect of AS101 on homocysteine, we performed several *in vitro* assays in which homocysteine

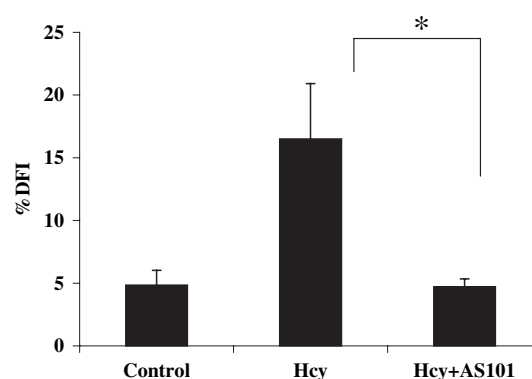


Fig. 5. AS101 abrogated homocysteine-induced sperm cell DNA degradation. Groups of C57BL/6 mice were given D,L-homocysteine ($200 \text{ mg}\cdot\text{kg}^{-1}\cdot\text{day}^{-1}$) in their drinking water, or given plain water. Mice were injected with either NaCl/P_i ($n = 8$) or AS101 ($1.5 \mu\text{g}\cdot\text{g}^{-1}$) ($n = 8$) every other day during the homocysteine administration period of 8 weeks. Following this, mice were killed with excess CO₂. DNA fragmentation was analyzed in sperm cells recovered from motile spermatozoa of treated mice. In the SCSA, DFI was calculated for spermatozoon in a sample, and the results were expressed as percentage of cells with abnormally high DFI (%DFI). DFI values were measured within a range of 0 and 1024 channels of fluorescence. * $P < 0.05$. The data shown represent the average of three separate experiments performed in duplicate, and error bars indicate the SD.

was allowed to react with IgG in the presence or absence of AS101 (Fig. 3E). Homocysteine caused a dose-dependent reduction of disulfide bonds in IgG, probably by interfering with the disulfide bonds between the heavy and light chains. Analysis of the supernatant of the above reaction for free thiol (–SH) groups using Ellman's reaction [33] (with the quantitative Nbs₂ reagent) revealed that whereas two homocysteine molecules had two thiol (–SH) groups, the RP in the same molar equivalent had no free –SH groups (Fig. 3C). This reaction was rapid and occurred within minutes (Fig. 3D), suggesting a mechanism in which two homocysteine molecules combined to form a single homocysteine molecule through a disulfide bond.

Fig. 3. (A) Raman spectrum of homocysteine. A Raman spectrum ($0\text{--}4000 \text{ cm}^{-1}$) of D,L-homocysteine was obtained. The S–H bond ($2550\text{--}2600 \text{ cm}^{-1}$) is labeled. (B) S–S bond in the Raman spectrum of the RP of AS101 and homocysteine. Raman spectrum ($0\text{--}4000 \text{ cm}^{-1}$) of RP; the S–S bond ($430\text{--}550 \text{ cm}^{-1}$) is labeled. (C) The RP of AS101 and homocysteine lacks the free thiol (–SH) group, in contrast to homocysteine. D,L-Homocysteine (1.94 mM) dissolved in NaCl/P_i was incubated with or without AS101 (0.318 mM in NaCl/P_i) on a rotating plate overnight at 37°C . Nbs₂ was then added, and allowed to react for 15 min; the colored RP was read at 412 nm . * $P < 0.05$. (D) AS101 reacts rapidly with homocysteine. D,L-Homocysteine (1.94 mM) dissolved in NaCl/P_i was incubated with or without AS101 (0.318 mM in NaCl/P_i) for 2 min. Free –SH groups were measured at 0, 1 and 2 min after the addition of AS101. Nbs₂ was then added, and allowed to react for 15 min; the RP was read at 412 nm . * $P < 0.05$. (E) IgG disassembly by D,L-homocysteine was abrogated by AS101. D,L-Homocysteine cleaved IgG in a dose-dependent manner, as seen in the elevated heavy-chain fragment in the left panel. Addition of AS101 ($2.5 \mu\text{g}\cdot\text{mL}^{-1}$) reduced this effect (right panel, middle lane). (F) High-resolution MS analysis of the RP indicated an M_r of 267.049 along with the lower molecular weight products, the result of the breakage of the molecule in this method. The M_r of the RP is tagged with an asterisk (*). Error bars represent the SD from three different experiments in duplicate.

To further evaluate the reaction of AS101 with homocysteine, we analyzed homocysteine and its RP using Raman spectroscopy. Raman spectroscopy provides vibrational information that is very specific for the chemical bonds in molecules. Whereas homocysteine demonstrated a peak corresponding to an S–H bond (Fig. 3A), the RP lost this bond and a new S–S bond was formed (Fig. 3B). NMR also indicated that the structure of the RP included a disulfide bond involving two homocysteine molecules. Finally, mass spectrum analysis led to the conclusion that the RP's M_r was equal to that of homocystine (Fig. 3).

The demonstration that AS101, as an organotellurium compound, can react with homocysteine to produce homocystine is important, as the conversion of homocysteine to homocystine and/or other disulfide mixtures and its renal clearance in the urine is known to be a major nontoxic secretion pathway of homocysteine from the body [34]. We next sought to analyze whether this effect also occurred *in vivo*. To mimic hyperhomocysteinemia in mice, we utilized the oral administration model of D,L-homocysteine. In this model, animals were fed D,L-homocysteine that had been added to their drinking water for a duration of 2 months. This resulted in high circulatory levels of homocysteine (Fig. 4A), but did not affect total cysteine levels (Fig. 4B). AS101 treatment administered to homocysteine-fed animals led to a reduction in total homocysteine but not total cysteine levels (Fig. 4A,B, respectively). It remains to be elucidated whether a degree of specificity for different thiols exists for AS101 *in vivo*.

The AS101 concentration used by us in the cell culture experiments ($2.5 \mu\text{g}\cdot\text{mL}^{-1}$) and the *in vivo* experiments ($1.5 \mu\text{g}\cdot\text{g}^{-1}$) correlated with the circulatory levels of plasma tellurium measured during chronic systemic AS101 administration to dogs in a previous pharmacokinetic study (unpublished results).

Subfertility has been very recently associated with hyperhomocysteinemia [17], whereas homocysteine was shown to be inversely associated with fertility outcome. The reason for this, however, is obscure. To the best of our knowledge, our results demonstrate a novel mechanism by which even moderate ($22.36 \pm 7.47 \mu\text{M hcy}$) hyperhomocysteinemia in mice can induce infertility by causing aberrant DNA structures and increased DNA fragmentation in sperm cells, as illustrated in Fig. 5. This correlates with the DNA damage caused by homocysteine, as sperm cells, as constantly dividing cells, are very sensitive to such damage. These findings should be further investigated in human subjects to try to find reasons for unexplained fertility problems observed in men.

In this study, we unraveled another aspect of the biology of tellurium by showing that the organotellurium

compound AS101 reacted with homocysteine. The mechanism for this activity was chemical modification of homocysteine to homocystine. This mechanism may also be involved in the reduction of circulatory levels of homocysteine by AS101 *in vivo*. However, we do not rule out additional mechanisms that may be responsible for the lowering of total homocysteine levels by AS101 *in vivo*. Our hyperhomocysteinemia model revealed a novel mechanism by which homocysteine damaged the DNA structure of sperm cells, thus causing infertility. This effect was completely abrogated by AS101. The novel mechanism of the reaction between AS101, a nontoxic organotellurium compound, and homocysteine may be of clinical importance, as it might reduce homocysteine levels in patients, irrespective of the cause of hyperhomocysteinemia.

Experimental procedures

Materials

D,L-Homocysteine and propidium iodide (PI) were purchased from Sigma (St Louis, MO, USA). The caspase-3 colorimetric substrate, Ac-benzyloxycarbonyl aspartyl glutamylvalyl-aspartic acid (DEVD)-*p*-nitroaniline (pNA), was purchased from Bachem AG (Bubendorf, Switzerland). Fetal bovine serum, RPMI-1640, penicillin and streptomycin were purchased from Gibco Laboratories (Grand Island, NY, USA). Caspase-3 and PARP1 antibodies were purchased from Cell Signaling (Danvers, MA, USA). Antibody against α -tubulin was purchased from Sigma. AS101 was synthesized by M Albeck (Department of Chemistry, Bar-Ilan University) in NaCl/P_i (pH 7.4), and maintained at 4 °C.

Cell culture

HL-60, a human promyelocytic cell line, was cultured in RPMI-1640 supplemented with 10% heat-inactivated fetal bovine serum and antibiotics ($2000 \text{ U}\cdot\text{L}^{-1}$ penicillin and $20 \text{ mg}\cdot\text{L}^{-1}$ streptomycin). Cell cultures were maintained in a humidified 5% CO₂ atmosphere at 37 °C.

Caspase-3 enzymatic activity

Cells (1×10^6) were incubated with cold lysis buffer for 10 min. Cell lysate containing 50 μg of protein was added to 148 μL of reaction buffer ($100 \text{ mmol}\cdot\text{L}^{-1}$ Hepes, pH 7.5, 20% glycerol, $0.5 \text{ mmol}\cdot\text{L}^{-1}$ EDTA, and $5 \text{ mmol}\cdot\text{L}^{-1}$ dithiothreitol) and 50 μM caspase-3 colorimetric substrate, DEVD-pNA. Samples were incubated at 37 °C for 6 h in a 96-well flat-bottomed microplate. Color was read using a Bio-Rad model 680 microplate reader (Bio-Rad Laboratories, Hercules, CA, USA) at a wavelength of 405 nm.

Analysis of apoptotic cells with hypodiploid DNA contents

Cells were collected, washed with Ca^{2+} -free and Mg^{2+} -free NaCl/P_i , and fixed in ice-cold 70% ethanol overnight. Cells were then incubated with PI buffer [PI ($50 \mu\text{g}\cdot\text{mL}^{-1}$), 0.1% sodium citrate, 0.1% Triton X-100 and $0.2 \text{ mg}\cdot\text{mL}^{-1}$ RNaseA in Ca^{2+} -free and Mg^{2+} -free NaCl/P_i] for 30 min at 4°C . Samples were analyzed using FacsCalibur (Becton-Dickinson, Mountain View, CA, USA). The percentage of cells in different cell cycle phases was estimated from PI histograms using the MODFIT 2.8 program (Coulter Verity, Topsham, ME, USA). Hypodiploid cells, i.e. those with sub- G_0/G_1 DNA contents, were defined as apoptotic cells, as described by Endresen *et al.* [27].

Western blotting

Protein concentration was quantified using Bradford reagent (Bio-Rad). Samples were then electrophoresed using 10% separating gel and 4% stacking SDS polyacrylamide gels (SDS/PAGE) according to Laemmli [39]. Gels were then electroblotted using semidry transfer apparatus (Bio-Rad) in transfer buffer containing 0.025 M Tris base, 0.15 M glycine and 10% (v/v) methanol for 1.5 h at 15 V onto nitrocellulose membranes (Bio-Rad). The membranes were then incubated in blocking buffer (5% nonfat milk in 20 mM Tris/HCl, pH 7.5, 137 mM NaCl, 0.2% Tween-20) for 1 h at room temperature. Membranes were incubated overnight at 4°C with the indicated antibody. After being washed three times (5 min per wash) with NaCl/Tris-T (20 mM Tris/HCl, pH 7.5, 137 mM NaCl, 0.2% Tween-20), the membrane was incubated with a horseradish peroxidase-conjugated secondary antibody. After being washed five times (5 min per wash) with NaCl/Tris-T, the membrane was incubated with the chemoluminescent substrate ECL (Pierce-Endogen, Rockford, IL, USA) for 5 min, and chemoluminescence signals were visualized by exposing the membrane to X-ray film (Kodak X-ray film; InterScience, Mississauga, Ontario, Canada).

Raman analysis

D,L-Homocysteine and other reaction products were analyzed using a Raman division instrument (Jobin Yvon Horiba, Edison, NJ, USA). Data were collected with the $\lambda = 514.532 \text{ nm}$ line of an argon laser as the excitation source at ambient temperature in the range $100\text{--}4000 \text{ cm}^{-1}$, with an $1800 \text{ g}\cdot\text{mm}^{-1}$ grating and a $100\times$ objective.

NMR analysis

NMR spectra of D,L-homocysteine and other RPs were recorded with an AC Bruker 200 instrument (Rheinstetten,

Germany). The RP of AS101 and homocysteine was centrifuged using SpeedVac at max. speed plus model SC110A (Savant Instruments, Holbrook, NY, USA) under vacuum (VacuuBrand diaphragm vacuum pump model MZ-2C; Wertheim, Germany), to complete dryness. Compounds were characterized by ^1H -NMR. ^1H -NMR spectra were recorded at 300 MHz in D_2O . Chemical shifts were reported in the δ scale. Calculated p.p.m. values for both homocysteine and homocystine were obtained using CHEMDRAW ULTRA 9.0 software in the CHEMOFFICE 2005 bundle (<http://www.cambridgesoft.com/>).

Mass spectra

High-resolution mass spectrum analysis was performed using VG Autospec Micromass (Waters, Milford, MA, USA) with CI^+ (chemical ionization)/ CH_4 ionization.

Homocysteine quantification

Blood samples were kept in ice-cooled EDTA tubes. Plasma was separated by centrifugation at $1500 g$ at 5°C and stored at -20°C . Total homocysteine levels were measured by HPLC with fluorescence detection, following labeling of homocysteine with monobromobimane, according to a modification of the method of Araki & Sako [28]. In brief, disulfide bonds were reduced using sodium borohydride (final concentration 0.4 M) instead of tri-*n*-tributylphosphine, and free $-\text{SH}$ residues were derivatized using the thiol-specific reagent monobromobimane (final concentration 0.102 M) instead of the fluorogenic reagent ammonium 7-fluorobenzo-2-oxa-1,3-diazole-4-sulfonate.

Quantitative determination of sulfhydryl ($-\text{SH}$) groups

A stock solution of 50 mM Nbs_2 was prepared in double-deionized water (ddw)/ethanol (5 : 3 v/v) solution. The Nbs_2 working solution contained 2 mM Nbs_2 and 20 mM sodium acetate. For the Ellman assay, $5 \mu\text{L}$ of sample was added to $25 \mu\text{L}$ of Nbs_2 working solution, followed by $420 \mu\text{L}$ of ddw and $50 \mu\text{L}$ of 1 M Tris buffer (pH 8). After incubation for 15 min, absorbance was measured at 412 nm using a Bio-Rad model 680 microplate reader.

SDS/PAGE to detect IgG cleavage products

Rabbit IgG ($1 \mu\text{g}$) was incubated overnight with different concentrations of homocysteine and/or AS101 in NaCl/P_i on a rotating plate at 37°C . Loading buffer, without SDS, was then added to the samples. SDS/PAGE was performed according to Laemmli [39], with 10% separating gel and 4% stacking gel. Electrophoresis was performed under constant

current. Proteins were detected by silver staining. The following washings were done: one washing (30 min) in 50% methanol and 12% acetic acid; two washings (10 min each) in 10% ethanol and 5% acetic acid; one washing (10 min) in 3.4 mM $K_2Cr_2O_7$ and 3.2 mM HNO_3 ; four washings (30 s each) in ddw; one washing (30 min) in 12 mM $AgNO_3$ under lamp illumination; washing in ddw; very fast washing in 0.28 mM Na_2CO_3 and 1% formaldehyde; and washing in ddw and store-developed gel in 1% acetic acid.

Animals used for experiments

Eight-week-old male C57bL/6 mice were purchased from Harlan Laboratories (Jerusalem, Israel). Animal experiments were performed in accordance with institutional protocols, and approved by the Animal Care and Use Committee of Bar-Ilan University.

Hyperhomocysteinemic mouse model

C57bL/6 mice were given homocysteine ($200\text{ mg}\cdot\text{kg}^{-1}\cdot\text{day}^{-1}$) in their drinking water, and injected with either $NaCl/P_i$ ($n = 8$) or AS101 ($1.5\text{ }\mu\text{g}\cdot\text{g}^{-1}$) ($n = 8$) every other day for 8 weeks. Following this, the mice were killed with excess CO_2 , and blood plasma was removed.

Recovery of testis tissues

In order to recover the motile spermatozoa, the epididymides were minced with fine scissors and incubated at $37\text{ }^\circ\text{C}$ (95% air, 5% CO_2) for 15 min in 1 mL of M2 medium (Sigma). Aliquots of the sperm present in the supernatant were fixed for sperm chromatin structure assay (SCSA) analysis.

SCSA

Sperm aliquots were washed twice with cold TNE buffer solution (0.01 M Tris, 0.15 M NaCl, 0.001 M EDTA, pH 7.4) and centrifuged at 400 g for 20 min at $4\text{ }^\circ\text{C}$ (Sigma 2–5 centrifuge, ATR, Laurel, MD, USA). The final pellet was resuspended in 0.1 mL of TNMg buffer (0.02 M Tris, 0.15 M NaCl, 0.005 M $MgCl_2$, pH 7.4), and then fixed by forceful pipetting into 0.9 mL of an acetone/70% ethanol (1 : 1 v/v) solution. All steps of this procedure were performed at $4\text{ }^\circ\text{C}$. Sperms were stained with acridine orange as previously described [29]. Fixed sperm aliquots were diluted in TNE buffer (0.15 M NaCl, 0.001 M EDTA, 0.01 M Tris, pH 7.4) to a final concentration of $1\text{--}2 \times 10^6\text{ cells}\cdot\text{mL}^{-1}$. Then, 200 μL of sperm was added to 400 μL of a detergent/acid solution consisting of 0.1% Triton X-100 in 0.08 M HCl and 0.15 M NaCl (pH 1.4). After 30 s, 1.2 mL of staining solution containing $6\text{ mg}\cdot\text{mL}^{-1}$ electrophoretically purified acridine orange in staining buffer (prepared by mixing 370 mL of 0.1 M citric acid mono-

hydrate and 630 mL of 0.2 M Na_2HPO_4 and adding 0.372 g of disodium EDTA and 8.77 g of NaCl, pH 7.4) was added to the sample. Flow cytometry was measured according to the method of Evenson *et al.* [40] using a FacsCalibur (Becton-Dickinson) flow cytometer equipped with ultrasense and a 15 mW argon ion laser with an excitation wavelength of 488 nm. The internal standard for calibration was a stock of fixed ram sperm nuclei prepared as described earlier. For each sample, 10^3 cells were analyzed. The percentage DNA fragmentation index (DFI) was calculated using a RATIO TIME 1.1 software package (Becton-Dickinson).

Statistical analysis

The results were analyzed using a two-tailed independent Student's *t*-test. Statistical significance was defined as $P < 0.05$.

Acknowledgements

The research described in this article was partly supported by the Milton and Lois Shiffman Global Research Program and by the Safdié Institute for AIDS and Immunology Research. Part of the research was conducted by Eitan Okun, in partial fulfillment of the requirements for a PhD degree, and by Yahav Dikshtein, in partial fulfillment of the requirements for an MSc degree, both at Bar-Ilan University.

References

- 1 Lentz SR (2005) Mechanisms of homocysteine-induced atherothrombosis. *J Thromb Haemost* **3**, 1646–1654.
- 2 Seshadri S, Beiser A, Selhub J, Jacques PF, Rosenberg IH, D'Agostino RB, Wilson PW & Wolf PA (2002) Plasma homocysteine as a risk factor for dementia and Alzheimer's disease. *N Engl J Med* **346**, 476–483.
- 3 Ravaglia G, Forti P, Maioli F, Martelli M, Servadei L, Brunetti N, Porcellini E & Licastro F (2005) Homocysteine and folate as risk factors for dementia and Alzheimer disease. *Am J Clin Nutr* **82**, 636–643.
- 4 Miller JW (2002) Homocysteine, folate deficiency, and Parkinson's disease. *Nutr Rev* **60**, 410–413.
- 5 Frosst P, Blom HJ, Milos R, Goyette P, Sheppard CA, Matthews RG, Boers GJ, den Heijer M, Kluijtmans LA, van den Heuvel LP *et al.* (1995) A candidate genetic risk factor for vascular disease: a common mutation in methylenetetrahydrofolate reductase. *Nat Genet* **10**, 111–113.
- 6 Jhee KH & Kruger WD (2005) The role of cystathionine beta-synthase in homocysteine metabolism. *Antioxid Redox Signal* **7**, 813–822.
- 7 Bailey LB (1998) Dietary reference intakes for folate: the debut of dietary folate equivalents. *Nutr Rev* **56**, 294–299.

- 8 Tucker KL, Rich S, Rosenberg I, Jacques P, Dallal G, Wilson PW & Selhub J (2000) Plasma vitamin B-12 concentrations relate to intake source in the Framingham Offspring study. *Am J Clin Nutr* **71**, 514–522.
- 9 Leklem JE (1990) Vitamin B-6: a status report. *J Nutr* **120** (Suppl. 11), 1503–1507.
- 10 Nygard O, Vollset SE, Refsum H, Stensvold I, Tverdal A, Nordrehaug JE, Ueland M & Kvale G (1995) Total plasma homocysteine and cardiovascular risk profile. The Hordaland Homocysteine Study. *JAMA* **274**, 1526–1533.
- 11 Nygard O, Refsum H, Ueland PM, Stensvold I, Nordrehaug JE, Kvale G & Vollset SE (1997) Coffee consumption and plasma total homocysteine: The Hordaland Homocysteine Study. *Am J Clin Nutr* **65**, 136–143.
- 12 Hultberg B, Berglund M, Andersson A & Frank A (1993) Elevated plasma homocysteine in alcoholics. *Alcohol Clin Exp Res* **17**, 687–689.
- 13 Kang SS, Wong PW, Glickman PB, MacLeod CM & Jaffe IA (1986) Protein-bound homocyst(e)ine in patients with rheumatoid arthritis undergoing D-penicillamine treatment. *J Clin Pharmacol* **26**, 712–715.
- 14 Hultberg B, Andersson A, Masson P, Larson M & Tunek A (1994) Plasma homocysteine and thiol compound fractions after oral administration of N-acetylcysteine. *Scand J Clin Lab Invest* **54**, 417–422.
- 15 Dechant KL, Brogden RN, Pilkington T & Faulds D (1991) Ifosfamide/mesna. A review of its antineoplastic activity, pharmacokinetic properties and therapeutic efficacy in cancer. *Drugs* **42**, 428–467.
- 16 Kelly TL, Neaga OR, Schwahn BC, Rozen R & Trasler JM (2005) Infertility in 5,10-methylenetetrahydrofolate reductase (MTHFR)-deficient male mice is partially alleviated by lifetime dietary betaine supplementation. *Biol Reprod* **72**, 667–677.
- 17 Ebisch IM, Peters WH, Thomas CM, Wetzels AM & Peer PG (2006) Steegers-Theunissen RP: homocysteine, glutathione and related thiols affect fertility parameters in the (sub) fertile couple. *Hum Reprod* **21**, 1725–1733.
- 18 Strassmann G, Kambayashi T, Jacob CO & Sredni B (1997) The immunomodulator AS-101 inhibits IL-10 release and augments TNF alpha and IL-1 alpha release by mouse and human mononuclear phagocytes. *Cell Immunol* **176**, 180–185.
- 19 Kalechman Y, Zuloff A, Albeck M, Strassmann G & Sredni B (1995) Role of endogenous cytokine secretion in radioprotection conferred by the immunomodulator ammonium trichloro(dioxyethylene-O-O') tellurate. *Blood* **85**, 1555–1561.
- 20 Kalechman Y, Sredni B, Weinstein T, Freidkin I, Tobar A, Albeck M & Gafter U (2003) Production of the novel mesangial autocrine growth factors GDNF and IL-10 is regulated by the immunomodulator AS101. *J Am Soc Nephrol* **14**, 620–630.
- 21 Rosenblatt-Bin H, Kalechman Y, Vonsover A, Da Xu RHJP, Shalit F, Huberman M, Klein A, Strassmann G, Albeck M & Sredni B (1998) The immunomodulator AS101 restores T(H1) type of response suppressed by *Babesia rodhaini* in BALB/c mice. *Cell Immunol* **184**, 12–25.
- 22 Kalechman Y, Gafter U, Albeck M, Alarcon-Segovia D & Sredni B (1997) Delay in the onset of systemic lupus erythematosus following treatment with the immunomodulator AS101: association with IL-10 inhibition and increase in TNF-alpha levels. *J Immunol* **159**, 2658–2667.
- 23 Kalechman Y, Gafter U, Gal R, Rushkin G, Yan D, Albeck M & Sredni B (2002) Anti-IL-10 therapeutic strategy using the immunomodulator AS101 in protecting mice from sepsis-induced death: dependence on timing of immunomodulating intervention. *J Immunol* **169**, 384–392.
- 24 Sredni B, Tichler T, Shani A, Catane R, Kaufman B, Strassmann G, Albeck M & Kalechman Y (1996) Pre-dominance of TH1 response in tumor-bearing mice and cancer patients treated with AS101. *J Natl Cancer Inst* **88**, 1276–1284.
- 25 Sredni B, Caspi RR, Klein A, Kalechman Y, Danziger Y, Ben Ya'akov M, Tamari T, Shalit F & Albeck M (1987) A new immunomodulating compound (AS-101) with potential therapeutic application. *Nature* **330**, 173–176.
- 26 Albeck HW, Sredni B & Albeck M (1998) Tellurium compounds. Selective inhibitors of cysteine proteases and model reaction with thiols. *Inorg Chem* **37**, 1904–1912.
- 27 Endresen PC, Prytz PS, Lysne S & Aarbakke J (1994) Homocysteine increases the relative number of apoptotic cells and reduces the relative number of apoptotic bodies in HL-60 cells treated with 3-deazaadenosine. *J Pharmacol Exp Ther* **269**, 1245–1253.
- 28 Araki A & Sako Y (1987) Determination of free and total homocysteine in human plasma by high-performance liquid chromatography with fluorescence detection. *J Chromatogr* **422**, 43–52.
- 29 Evenson D & Jost L (1987) Sperm chromatin structure assay is useful for fertility assessment. *Methods Cell Sci* **22**, 169–189.
- 30 Huang RF, Huang SM, Lin BS, Hung CY & Lu HT (2002) N-Acetylcysteine, vitamin C and vitamin E diminish homocysteine thiolactone-induced apoptosis in human promyeloid HL-60 cells. *J Nutr* **132**, 2151–2156.
- 31 Ventura P, Panini R, Abbati G, Marchetti G & Salvioli G (2003) Urinary and plasma homocysteine and cysteine levels during prolonged oral N-acetylcysteine therapy. *Pharmacology* **68**, 105–114.
- 32 Gonzalez S, Huerta JM, Alvarez-Uria J, Fernandez S, Patterson AM & Lasheras C (2004) Serum selenium is

- associated with plasma homocysteine concentrations in elderly humans. *J Nutr* **134**, 1736–1740.
- 33 Ellman GL (1959) Tissue sulfhydryl groups. *Arch Biochem Biophys* **82**, 70–77.
- 34 Bilwani F, Syed NA, Usman M & Khurshid M (2005) Familial homocysteinuria. *J Coll Physicians Surg Pak* **15**, 106–107.
- 35 Refsum H, Helland S & Ueland PM (1985) Radioenzymic determination of homocysteine in plasma and urine. *Clin Chem* **31**, 624–628.
- 36 Foreman JW, Wald H, Blumberg G, Pepe LM & Segal S (1982) Homocystine uptake in isolated rat renal cortical tubules. *Metabolism* **31**, 613–619.
- 37 Arkowska A & Wojciechowski W (1987) Spectroscopic and magnetic properties of complex compounds of nickel(II) with homocysteine and homocystine. *Pol J Chem* **61** (4–6), 649–651.
- 38 Van Wart HE & Scheraga HA (1976) Raman spectra of cystine-related disulfides. Effect of rotational isomerism about carbon–sulfur bonds on sulfur–sulfur stretching frequencies. *J Phys Chem* **80**, 1812–1822.
- 39 Laemmli UK (1970) Cleavage of structural proteins during the assembly of the head of bacteriophage T4. *Nature* **15**, 680–685.
- 40 Evenson DP, Darzynkiewicz Z & Melamed MR (1980) Relation of mammalian sperm chromatin heterogeneity to fertility. *Science* **210** (4474), 1131–1133.
- 41 Sredni B, Geffen-Aricha R, Duan W, Albeck M, Shalit F, Lander HM, Kinor N, Sagi O, Albeck A, Yosef S *et al.* (2007) Multifunctional tellurium molecule protects and restores dopaminergic neurons in Parkinson's disease models. *FASEB J* (in press).
- 42 Okun E, Arumugam TV, Tang S-C, Gleichmann M, Albeck M, Sredni B & Mattson MP (2007) The organo-tellurium compound ammonium trichloro(dioxoethylene-O O') tellurate (AS101) enhances neuronal survival and improves functional outcome in an ischemic stroke model in mice. *NeuroChem J* (in press).